ORIGINAL ARTICLE

Ultrastructural analysis of prefrontal cortical inputs to the rat amygdala: spatial relationships to presumed dopamine axons and D1 and D2 receptors

Aline Pinto · Susan R. Sesack

Abstract Projections from the prefrontal cortex (PFC) to the amygdala (AMG) regulate affective behaviors in a manner that is modulated by dopamine (DA). Although PFC and DA inputs overlap within the basolateral nucleus (BLA) and intercalated cell masses (ICMs), the spatial relationship between these afferents has not been investigated, nor is it known how DA D1 (D1R) and D2 (D2R) receptors are localized in relationship to PFC terminals. We therefore combined tract-tracing from the rat PFC to the AMG with immunocytochemical labeling of tyrosine hydroxylase (TH) to identify presumed DA axons or D1R and D2R. In both the ICMs and BLA, PFC terminals formed asymmetric synapses onto spines that typically did not receive secondary synaptic inputs. TH-immunoreactive (-ir) fibers in the adjacent neuropil typically contacted different structures. Although PFC and TH-ir axons were sometimes apposed to the same dendrites or to each other, PFC terminals only rarely synapsed onto dendrites that also received synapses from TH-ir axons. D1R-ir spines and dendrites were observed commonly within the ICMs but less frequently within the BLA, and PFC axons in the ICMs occasionally synapsed onto D1R-ir spines. Within both regions, D2R-ir spines, dendrites, and axons were observed. PFC terminals occasionally contained presynaptic labeling for D2R but were not observed to synapse onto D2R-ir targets. The infrequent observation of synaptic convergence between PFC and presumed DA terminals within the AMG suggests that DA modulates PFC inputs primarily via extrasynaptic mechanisms, a conclusion supported by the localization of D2R within and D1R postsynaptic to PFC terminals.

Introduction

The amygdala (AMG) has been implicated in the formation of phobias and anxiety (Davidson 2002; Davis 2000; Le-Doux 2000), and dysfunctions within this region, as well as the prefrontal cortex (PFC) have been observed in patients with affective disorders and schizophrenia (Drevets 2003; Grace and Rosenkranz 2002; Rauch et al. 2003). Interactions between the PFC and the AMG are necessary for the guidance of appropriate behavioral responses (Baxter et al. 2000) and for the extinction of learned fear (Phelps et al. 2004). Moreover, neuronal activity within the PFC and the AMG seems to be reciprocally correlated (Garcia et al. 1999; Rosenkranz and Grace 2002b).

In the rat, the PFC projection to the AMG originates from layers II and V of the prelimbic (PL) and infralimbic (IL) regions (Pinto and Sesack 2000) and innervates most densely the basolateral area (BLA) and intercalated cell masses (ICMs) (Berretta et al. 2005; Cassell and Wright 1986; McDonald 1998; McDonald et al. 1996; Ottersen 1982; Sesack et al. 1989; Vertes 2004). Within the BLA, PFC terminals form asymmetric synapses primarily onto dendritic spines and less often onto distal dendritic shafts (Brinley-Reed et al. 1995). The synaptic organization of the PFC input to the ICMs has not yet been investigated.

Dopamine (DA) modulatory systems have also been implicated in affective behaviors. For example, the DA innervation of the AMG is particularly responsive to stress

A. Pinto · S. R. Sesack (✉)
Department of Neuroscience and Psychiatry,
University of Pittsburgh, 210 Langley Hall,
Pittsburgh, PA 15260, USA
e-mail: sesack@pitt.edu

(Inglis and Moghaddam 1999), and DA transmission in this area contributes to the acquisition and expression of Pavlovian fear conditioning (Guarraci et al. 1999; Lamont and Kokkinidis 1998). Moreover, alterations of DA activity within the AMG impair the recall of affect-charged memories (Nader and LeDoux 1999). Physiological recordings from AMG neurons indicate that DA mediates direct postsynaptic actions (Kröner et al. 2005; Lorétan et al. 2004; Marowsky et al. 2005; Pickel et al. 2006; Rosenkranz and Grace 1999) and also modulates neuronal responses to incoming stimuli during Pavlovian conditioning (Rosenkranz and Grace 2002a). Moreover, DA receptor activation attenuates neuronal responses to PFC inputs (Rosenkranz and Grace 1999, 2002b).

The anatomical substrate for such modulation is not yet clear. In other brain regions, DA is thought to modulate specific inputs by synapsing onto spines that also receive asymmetric, presumably excitatory glutamate contacts (Freund et al. 1984; Goldman-Rakic et al. 1989; Johnson et al. 1994; Sesack and Pickel 1990, 1992). Dopamine fibers from the ventral midbrain project throughout the AMG. Similar to the PFC projection, DA afferents are particularly dense within the ICMs and the BLA, but also provide a dense projection to the central nucleus (Ce) (Asan 1998; Brinley-Reed and McDonald 1999; Fallon and Ciofi 1992; Marowsky et al. 2005; Swanson 1982). Within these nuclei, DA terminals form primarily en passant symmetric type synapses onto small dendrites and spines (Asan 1997). Hence, convergent synapses by PFC and DA terminals onto common targets in the AMG could provide a substrate for specific DA modulation of PFC inputs to this region. However, such a convergent spatial relationship has not yet been examined by ultrastructural analyses.

In addition to its synaptic contacts, DA activates receptors outside of synaptic specializations (Descarries and Umbriaco 1995; Dumartin et al. 1998; Garris and Wightman 1994; Paspalas and Goldman-Rakic 2004; Sesack 2002). Hence, DA may also modulate PFC afferents to the AMG via extrasynaptic receptors localized to the PFC terminals or their targets. Various studies have demonstrated mRNA or immunoreactivity for the D1 (D1R) and D2 (D2R) receptors in several nuclei of the AMG (Asan 1998; Fremeau et al. 1991; Fuxe et al. 2003; Maltais et al. 2000; Meador-Woodruff et al. 1991; Pickel et al. 2006; Weiner et al. 1991). Moreover, both receptors play a role in behaviors mediated by this region. For example, either D1R or D2R antagonism within the AMG impairs conditioned fear acquisition (Greba et al. 2001; Greba and Kokkinidis 2000; Guarraci et al. (1999, 2000). D1 receptor activation has specifically been shown to attenuate PFC-evoked inhibition of BLA projection neurons (Rosenkranz and Grace 2002b), possibly through actions involving

reduced NMDA receptor transmission (Pickel et al. 2006) and/or inhibition of GABA tone (Marowsky et al. 2005).

These studies indicate the involvement of DA in the modulation of PFC inputs to the AMG. However, little is known regarding the spatial relationships between PFC afferents and DA terminals or D1R and D2R in this region. Hence, tract-tracing and immunocytochemical methods were combined to characterize the patterns of synaptic connectivity formed by PFC and DA terminals within the BLA and the ICMs and to examine the spatial associations between PFC profiles and D1R and D2R. A preliminary account of this work has been previously published (Pinto and Sesack 2003).

Materials and methods

Tract-tracing

Eleven adult male Spraque Dawley rats weighing 300–400 g were used in this study. The animals were kept on a 12 h light/dark cycle and were provided with rat chow and water *ad libitum*. The subjects were anesthetized either with chloral hydrate (420 mg/kg, i.p.) or with a mixture of ketamine (34 mg/kg), acepromazine (1 mg/kg), and xylazine (7 mg/kg) injected i.m. The animals were placed in a stereotaxic apparatus and received bilateral injections of an anterograde tracer or bilateral electrolytic lesions of the medial PFC. All efforts were made to minimize the extent of discomfort during the experiments and the number of animals used. The anesthetic and surgical procedures used in this study followed the principles of laboratory animal care (NIH publication no. 86–23, revised 1985) and were approved by the Institutional Animal Care and Use Committee at the University of Pittsburgh.

Either biotinylated dextran amine (BDA; 10,000 molecular weight, Molecular Probes, Eugene, OR), dissolved as a 10% solution in 0.01 M phosphate buffered saline (PBS), or *Phaseolus vulgaris*-leucoagglutinin (PHAL, Vector Laboratories, Burlingame, CA), dissolved as a 2.5% solution in 0.01 M PBS, pH 8.0, was infused into the medial PFC of 8 animals at the following coordinates: 3.3 and 2.7 mm anterior to Bregma, 0.7 mm lateral to the midline sinus, and 4.4 and 5.0 mm ventral to the skull surface (Paxinos and Watson 1986). The tracers were delivered by iontophoresis through glass pipettes (tip diameter 50–75 μm for BDA or 25 μm for PHAL) using positive 5 μA current pulses, on and off every 10 s for 15 min.

Four animals received electrolytic lesions of the medial PFC at the following coordinates: 3.3 and 2.7 mm anterior to Bregma, 0.8 mm lateral to the midline, and 4.6 and, 5.5 mm ventral to the skull surface (Paxinos and Watson

1986). The lesions were produced by passing a 0.5 mA constant anodal current for 30 s through an epoxylite-coated stainless steel monopolar electrode exposed for 1.0 mm at the tip.

The three different tracer methods described above were employed in order to maximize the advantages of each approach. BDA and PHA-L were used for their excellent uptake and transport dynamics (Wouterlood and Jorritsma-Byham 1993), although the BDA method prevented the use of the more sensitive avidin-biotin peroxidase (ABC) technique (Hsu et al. 1981) to label TH or DA receptors (see below). The use of the electrolytic lesion method was expected to alter the normal morphology of PFC axons and to prevent the detection of receptors within these profiles. However, anterograde degeneration is likely to label a larger population of PFC profiles within the AMG, based on the size of the lesion site and the occurrence of degeneration throughout the thickness of tissue sections (Sesack and Pickel 1992; Sesack et al. 2006). Moreover, the approach would allow TH and DA receptors to be detected by the ABC method. Hence, it is likely that the combined use of three different labeling techniques with similar results compensated for the limitations inherent to each individual method.

Perfusion

The appropriate survival time for animals receiving electrolytic lesions was empirically determined to be 4 days following examination of tissue from animals that survived for 4 or 5 days. Animals with tracer injections survived 5 days for BDA or 10 days for PHAL. After the appropriate survival time, animals were anesthetized with sodium pentobarbital, 50 mg/kg, i.p. Animals receiving tracer injections also received an i.p. injection of the zinc chelator, sodium diethyl dithiocarbamate (1 g/kg, Sigma, St Louis, MO) (Veznedaroglu and Milner 1992) 15 min prior to the perfusion in order to eliminate spurious silver labeling due to the presence of zinc. The animals were then sacrificed by perfusion through the aorta with 10 ml of 1,000 U/ml heparin saline, followed by 50 ml of 3.75% acrolein (Electron Microscopy Sciences, Hatfield, PA) in 2% paraformaldehyde and 250 ml of 2% paraformaldehyde in 0.1 M phosphate buffer, pH 7.4 (PB). The brains were removed, cut into 4–5 mm blocks, and post-fixed in 2% paraformaldehyde for 30 min. Blocks containing the PFC or the AMG were sectioned at 50 μm in PB using a vibratome. Sections were incubated in 1% sodium borohydride (Sigma) for 30 min, then rinsed in PB followed by rinses in 0.1 M tris-buffered saline, pH 7.6 (TBS), followed by a 30 min incubation at room temperature in a blocking solution containing 1% bovine serum albumin, 0.04% Triton 100X, and 3% normal goat serum in TBS.

Immunocytochemical procedures

Presumed DA axons in the AMG were labeled by a monoclonal antibody directed against the catecholamine synthetic enzyme, tyrosine hydroxylase (TH; Chemicon International, Temecula, CA). The specificity of this antibody has been extensively described in prior publications (Lewis and Sesack 1997; Miner et al. 2003; Sesack et al. 1995; Wolf et al. 1991). Tyrosine hydroxylase is contained in both DA and norepinephrine neurons. However, the majority of axonal projections from norepinephrine cells to cortical regions contain undetectable levels of TH by either light or electron microscopy (Lewis and Sesack 1997; Miner et al. 2003), and similar observations have been made in the AMG using both methods (Asan 1997, 1993). Hence, we utilized TH immunostaining as a relatively selective marker of DA axons in the AMG, with the acknowledgement that it may have included a small population of norepinephrine fibers (Asan 1993, 1997, 1998).

In pilot studies, the use of immunogold-silver to label TH resulted in a considerable reduction in sensitivity that appeared more substantial then when this method was used to label tracers. We therefore consistently used immunoperoxidase to label TH and immunogold-silver to label BDA or PHAL. The D1R or D2R were also detected by immunoperoxidase. The specificity of the D1R antibody, directed against 97 amino acids from the C terminus, has been well documented by Western blots from transfected mammalian cell lines and brain tissue (Levey et al. 1993; Yung et al. 1995). The D2R antibody was raised against 28 amino acids from the third cytoplasmic loop of the human receptor and has been demonstrated to specifically recognize the D2R by preadsorption with the immunizing peptide and by Western blot analysis (Boundy et al. 1993; Wang and Pickel 2002). Both antibodies have been shown to produce no cross-reaction with other DA receptor subtypes.

Animals receiving BDA injections

Sections from animals receiving BDA injections were processed for detection of TH using the peroxidase anti-peroxidase (PAP) method (Ordronneau et al. 1981) and for BDA using a gold-conjugated antibody to identify this tracer prior to plastic embedding. The PAP method rather than the avidin-biotin peroxidase approach (Hsu et al. 1981) was chosen because the latter reagents would have bound to the biotin group on the tracer. Following borohydride treatment and incubation in blocking solution, sections through the AMG were incubated overnight in mouse anti-TH antibody (1:1,000), then rinsed in TBS and incubated for 1 h in donkey anti-mouse IgG (1:100, Jackson ImmunoResearch Laboratories, West Grove, PA),

followed by rinses in TBS and a 1 h incubation in mouse anti-peroxidase (1:100, Jackson). The sections were then re-incubated for 1 h in donkey anti-mouse IgG, rinsed in TBS, and re-incubated for 1 h in mouse anti-peroxidase (Ordronneau et al. 1981) followed by rinses in TBS. The peroxidase reaction was developed using a solution of 0.022% diaminobenzidine (DAB) and 0.003% hydrogen peroxide in TBS. The sections were rinsed in TBS followed by rinses in 0.01 M PBS, pH 7.4, and a 30 min incubation in washing buffer containing 0.8% BSA, 0.1% fish gelatin, and 3% normal goat serum in PBS. They were then incubated overnight in 1 nm gold-conjugated goat anti-biotin IgG (1:50, Ted Pella, Redding, CA). The sections were rinsed, and post-fixed with 2% glutaraldehyde in PBS for 10 min at room temperature. After extensive rinses in PBS, bound gold particles were enhanced by treatment with silver solution (Amersham, Piscataway, NJ) for an empirically determined time ranging from 5 to 8 min.

Animals receiving PHAL injections

In animals receiving PHAL injections, the presence of TH, D1R, or D2R immunoreactivity within axonal or dendritic profiles was detected by immunoperoxidase, whereas the tracer was detected using pre-embedding immunogold-silver. Briefly, sections were incubated overnight in one of three antibody combinations: (1) mouse anti-TH (1:1,000) and rabbit anti-PHAL (1:1,000, Vector), (2) rat anti-D1R (1:1,000, Sigma/RBI) and rabbit anti-PHAL, or (3) rabbit anti-D2R (1 μg/ml; Chemicon) and goat anti-PHAL (1:1,000, Vector). These sections were then rinsed in TBS followed by a 1 h incubation in biotinylated horse anti-mouse IgG (1:400, Vector) for tissue being immunostained for TH, biotinylated donkey anti-rat IgG (1:100, Vector) for tissue being immunostained for D1R, or donkey anti-rabbit IgG (1:200, Jackson, minimal cross-reaction with other species including goat) for tissue processed for D2R. The secondary antibody incubations were followed by rinses in TBS and a 30 min incubation in avidin-biotin peroxidase complex (ABC). Bound peroxidase was revealed as previously described. The sections were then rinsed in TBS followed by PBS before being incubated for 30 min in washing buffer and then overnight in gold-conjugated goat anti-rabbit IgG (1:50, Ted Pella) for the TH or D1R labeled tissue, or donkey anti-goat IgG (1:50, Electron Microscopy Sciences) for the D2R labeled tissue. The following day, the sections were rinsed and postfixed in glutaraldehyde, and the bound gold particles were enhanced by treatment with silver solution as described above.

The specificity of the secondary antibodies has been demonstrated previously using sections from which primary antibodies were omitted. The specificity of the gold conjugated anti-biotin antibody is evidenced by the absence of specific gold–silver labeling in regions that are not innervated by the PFC. For dual labeling studies, evidence that secondary antibodies specifically recognize their respective species and not other species is shown by the lack of dually labeled profiles in the sections labeled for biotin and TH, PHAL and TH, or PHAL and D1R and from the observation of dual labeling only in axons in sections reacted for PHAL and D2R.

### Animals receiving electrolytic lesions

Sections through the AMG were incubated overnight in mouse anti-TH (1:1,000), rat anti-D1R (1:1,000), or rabbit anti-D2R (1 μg/ml) antibodies. The sections were then rinsed in TBS and incubated at room temperature for 30 min in biotinylated horse anti-mouse IgG (1:400, Vector), donkey anti-rat IgG (1:100, Jackson) or goat anti-rabbit IgG (1:200, Jackson), respectively. This was followed by rinses in TBS and a 30 min incubation in ABC. The bound peroxidase was visualized using DAB as the chromogen.

Light microscopy

For BDA and PHAL tracers, every sixth section through the PFC and AMG was processed by ABC peroxidase and included 0.2% Triton X-100 in the blocking and incubation solutions. For most animals, a few sections through the AMG were labeled for tracer by peroxidase and for GABA by immunogold-silver (mouse anti-GABA, 1:2,000, Sigma). These sections were used to help determine the boundaries of the BLA and ICMs (see below), based on studies showing that the ICMs consist solely of GABA neurons occupying the paracapsular narrow band of fibers coursing between the basolateral complex and the Ce (Millhouse 1986). Sections for light microscopy were mounted onto glass slides and coverslipped. For animals receiving electrolytic lesions, every sixth section through the PFC was mounted onto glass slides and stained for Nissl substance before being coverslipped. The light microscopic images in Fig. 1 were acquired digitally and adjusted for exposure and contrast using Adobe Photoshop.

Electron microscopy

Sections prepared for electron microscopy were rinsed in PB, post-fixed in osmium tetroxide (2% solution in PB) for 1 h, and rinsed again in PB. These sections were then dehydrated in a graded series of alcohols and propylene oxide, and finally embedded in epon-812 resin (Electron Microscopy Sciences) and baked overnight at 60°C.
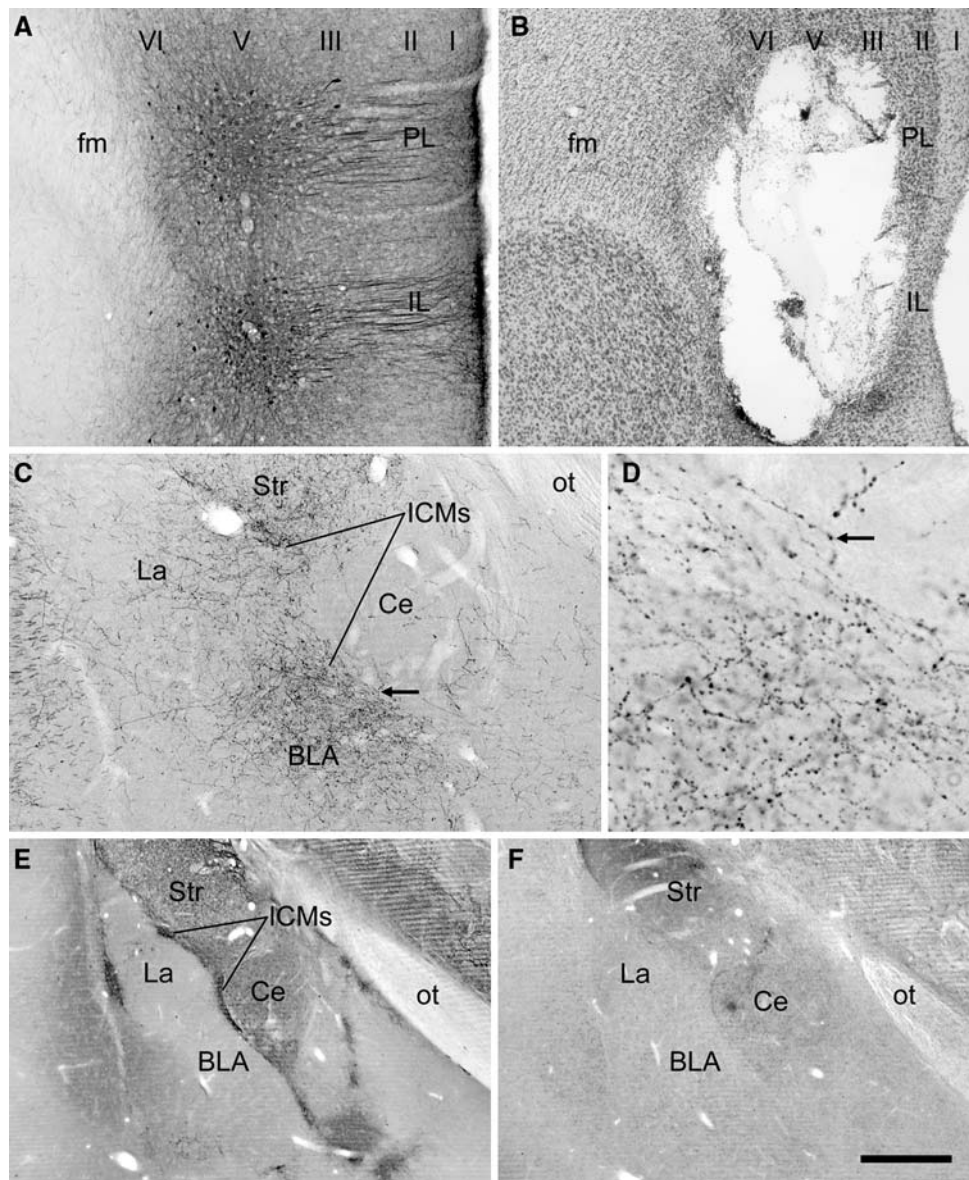
Fig. 1 Light micrographs showing representative injection and lesion sites in the rat PFC, anterograde transport to the AMG, and the distribution of D1 and D2 receptor immunoreactivity within the AMG. Panel **a** shows two PHAL injection sites centered in layer V of the PL and IL cortices. Panel **b** shows an electrolytic lesion of the PFC that involves most of the PL and IL as well as the medial portion of the forceps minor (fm). Panel **c** shows PHAL transport to the AMG from the injection site shown in panel **a**. The most dense fiber distribution involves the transition zone between the striatum (Str) and AMG, the ICMs, and the medial La and BLA. The Ce and regions lateral to the optic tract (ot) are relatively devoid of labeled fibers. Panel **d** shows PFC axons in the BLA at higher magnification and illustrates their branched and beaded morphology. *Arrows* in panels **c** and **d** indicate the same axon cluster. In panel **e**, dense immunostaining for the D1 receptor labels the narrow band between the Ce and the basolateral complex (La–BLA) that includes the ICMs. D1 immunostaining is also dense within the Ce and Str but is sparse within the La and BLA. In **f**, immunostaining for the D2 receptor in the AMG is noticeably less dense and more homogeneous than that seen for the D1 receptor. The Ce shows the highest levels of D2 labeling compared to other AMG nuclei. *Scale bar* shown in panel **f** represents 250 μm for panels **a** and **c**, 500 μm for panels **b**, **e**, and **f**, and 50 μm for panel **d**

Portions of the AMG including the ICMs and BLA were sectioned at 60–70 nm using an ultramicrotome (RMC, Tucson, AZ, USA). Ultrathin sections were collected onto copper mesh grids and counterstained with 5% uranyl acetate and Reynold's lead citrate.

Sampling

At least one section from each animal was examined, although in animals for which the tracer injections or electrolytic lesions produced optimal terminal labeling

within the AMG, up to three sections were examined. Immunoreaction product for TH and for the D2R was observed in both the ICMs and the BLA, the areas of the AMG showing the densest PFC terminal fields (Fig. 1). Consequently both regions were sampled in such sections, and the BLA sampling included primarily the dorsomedial portion of the anterior magnocellular division of this nucleus. The D1R immunostaining was found to be moderately heavy within the ICMs but considerably less dense within the BLA. Hence, examination of D1R labeled sections was concentrated within the ICMs.

Sections embedded in epon were photographed, and the area of interest within each section (BLA or ICMs) was determined by comparison to adjacent sections immunostained for GABA. The area of interest was drawn on the photographs, and the tissue was trimmed onto trapezoidal blocks at the same position and shape as drawn in the photographs. Tissue blocks were then cut at 70 nm and collected onto copper mesh grids.

Before high magnification electron microscopic examination of the tissue commenced, a careful drawing of the tissue trapezoid at low magnification was made onto a square grid notebook so that each square of the copper mesh grid was depicted. The location of each PFC terminal examined was then marked onto this grid map, which was then compared to the photographs of embedded tissue to determine whether each terminal was situated within the ICMs or BLA. For a few PFC terminals, their differential location within the ICMS or BLA could not be determined for certain (see results), and therefore, these profiles were not examined further. Moreover, the area of ICMs sampling may have included a small part of the lateral, paracapsular region of the Ce.

Data analysis

Tissue immunolabeled for TH

Within the BLA and the ICMs, all tracer-labeled or degenerating PFC profiles were counted, and the presence of TH-immunoreactive (-ir) profiles in the same microscopic field ($13.8 \ \mu m^2$ at $20,000 \times$ magnification) was registered. Photographs were made for every case in which PFC and TH-ir terminals were apposed to each other or formed synaptic or appositional contacts onto the same spines or dendrites. In the latter instances, these fields were also examined in 2–4 adjacent serial sections to determine whether synaptic features were present. Synaptic contacts were identified by clusters of vesicles at the presynaptic membrane, parallel arrangement of pre-and postsynaptic membranes, filamentous material within the synaptic cleft, and electron dense material at the postsynaptic membrane. The asymmetric synapses typically formed by PFC terminals exhibited larger zones of contact and thicker postsynaptic densities than the symmetric synapses usually established by TH-ir axons. Appositions were identified as points of contact between profiles that did not exhibit the synaptic characteristics described above. A total of $200,211 \ \mu m^2$ of tissue was examined. This area corresponds to the number of squares examined along the support grid, the approximate area encompassed by these squares ($3,025 \ \mu m^2$), and the approximate amount of tissue versus plastic in each square.

Tissue immunolabeled for the D1R and D2R

Every tracer-labeled or degenerating PFC profile was counted, and in each case it was determined whether D1R or D2R immunoreactivity was present within synaptic targets or within the tracer-labeled terminals themselves. Moreover, when PFC terminals were apposed to dendrites or spines immunoreactive for D1R or D2R, these fields were examined in 2–4 serial sections to determine whether PFC profiles formed synaptic contacts onto the receptor-labeled dendrites or spines. A total of $127,813 \ \mu m^2$ of tissue immunostained for D1R and $537,115 \ \mu m^2$ tissue immunostained for D2R was examined in the AMG.

Results

Light microscopic observations

The location of injection sites and the resulting patterns of anterograde labeling in the AMG were relatively similar in animals receiving PFC injections of either BDA or PHAL. Within the PFC, tracer injections usually targeted the deep layers V and VI of the PL and IL regions and extended for approximately 1.5 mm rostral to caudal (Fig. 1a). Numerous cell bodies containing tracer could be observed within these injection sites, and labeled dendrites ascended into superficial layers. The electrolytic lesions involved a larger portion of the PL and IL regions, extending approximately 2.2 mm rostral to caudal and covering superficial and deep layers of the PFC as well as the underlying white matter (Fig. 1b). Light microscopic examination of either PHAL or BDA transport to the AMG revealed a dense plexus of labeled fibers within the area encompassing the ICMs and the dorsomedial BLA (Fig. 1c). Labeled axons were extensively branched and displayed a densely beaded morphology (Fig. 1d). The lateral nucleus (La) received only moderate amounts of tracer, and the Ce outside the paracapsular region was largely avoided by PFC axons (Fig. 1c). Finally, it should be noted that a few retrogradely labeled cells in the AMG were seen when BDA was used as the tracer. However, these were typically observed
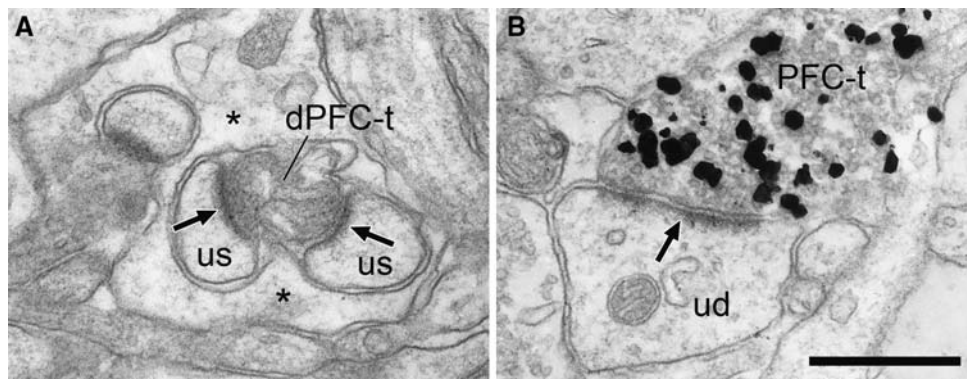
Fig. 2 Electron micrographs showing prefrontal cortical terminals (PFC-t) and their synaptic targets within the AMG. In panel **a**, a degenerating PFC-t (dPFC-t) within the ICMs forms asymmetric synaptic contacts (*black arrows*) onto two unlabeled spines (us). The dPFC-t and its postsynaptic targets are enveloped by glial processes (*asterisks*). In panel **b**, a PFC-t labeled by tracer within the BLA forms an asymmetric synapse (*black arrow*) onto a small unlabeled dendrite (ud). *Scale bar* represents 0.5 μm

ventral and caudal to regions containing maximal antero-grade transport.

Immunoperoxidase labeling for the D1R was heaviest within the ICMs, moderately dense within the Ce, and weakly present within the basolateral complex, particularly in the dorsomedial portions where PFC afferents are most dense (Fig. 1e). This highly patterned distribution matches previous descriptions for the D1R (Fuxe et al. 2003). The D2R was more evenly present within the various nuclei of the AMG, having an overall low density of staining and with the Ce expressing slightly heavier labeling than the other AMG nuclei (Fig. 1f).

Electron microscopic observations

PFC axons within the AMG

Electron microscopic examination of immunostained sections through the ICMs and BLA revealed numerous PFC axons or terminals undergoing degeneration following electrolytic lesions (Fig. 2a) or containing immunogold-silver labeling for BDA or PHAL following axonal transport (Fig. 2b). Soma or dendrites containing retrogradely transported BDA were not observed by electron microscopy. Terminals containing BDA or PHAL were readily identified by black immunogold-silver particles, whereas terminals undergoing degeneration were recognized by the presence of swollen mitochondria, disrupted vesicles, and an overall electron dense appearance (Peters et al. 1991; Sesack and Pickel 1992). In some cases, degenerating PFC terminals and their targets within the AMG were enveloped by glial processes (Fig. 2a). As detailed in Table 1, 161 PFC terminals were observed with the BLA or the ICMs. An additional 19 terminals that could not be confidently assigned to either the ICMs or BLA were not included in the analysis. Regardless of the method used for labeling, or the AMG nucleus examined, PFC terminals formed predominantly asymmetric synapses onto dendritic spines (93%, Fig. 2a), indicating that both tracers and lesions labeled similar axon populations. The remaining PFC terminals synapsed onto dendritic shafts (Fig. 2b).

PFC and TH-ir axons within the AMG

Many PFC terminals were observed in the neuropil adjacent to TH-ir axons (Figs. 3, 4; Table 1). In the majority of cases, these two profile types contacted separate targets (Fig. 3a, b). However, in some instances, PFC terminals

Table 1 PFC axons in the rat ICMs and BLA: association with TH+ profiles

	ICMs	BLA
Total number of PFC axons observed	76	85
Number (%) of PFC axons forming synapses in single sections	25/76 (33%)	19/85 (22%)
Number (%) of PFC axons observed in the same field[a] as TH+ profiles	56/76 (74%)	23/85 (27%)
Number (%) of PFC and TH+ profiles contacting common dendrites[b]	9/56 (16%)	4/23 (17%)
Number (%) of PFC and TH+ profiles directly apposed to each other	6/56 (11%)	1/23 (4%)

PFC prefrontal cortex, *ICMs* intercalated cell masses, *BLA* basolateral amygdala, *TH+* tyrosine hydroxylase immunoreactive

[a] Area of a micrograph at 20,000× magnification (13.8 μm²)

[b] Includes synapses and close appositions onto the same spine or dendrite

Fig. 3 Electron micrographs of PFC axons (PFC-a) and terminals (PFC-t) in the AMG and their spatial relationships to TH-ir axons (TH-a) and terminals (TH-t). PFC-ts occasionally form asymmetric synapses (*black arrows*) onto unlabeled spines (us) that are also contacted by TH axons, although junctional specializations are often absent at the latter sites of contact. In panel **a**, a PFC-t within the BLA synapses onto an unlabeled spine that is not contacted by a nearby TH-t. In panel **b**, a PFC-t within the ICMs synapses onto an unlabeled spine that is also contacted at its base by a TH-a. A nearby TH-t forms a symmetric synapse (*white arrow*) onto an unlabeled dendrite (ud). Panel **c** shows a PFC-t within the BLA in direct apposition (facing *arrowheads*) to a TH-a. *Scale bar* represents 0.5 μm
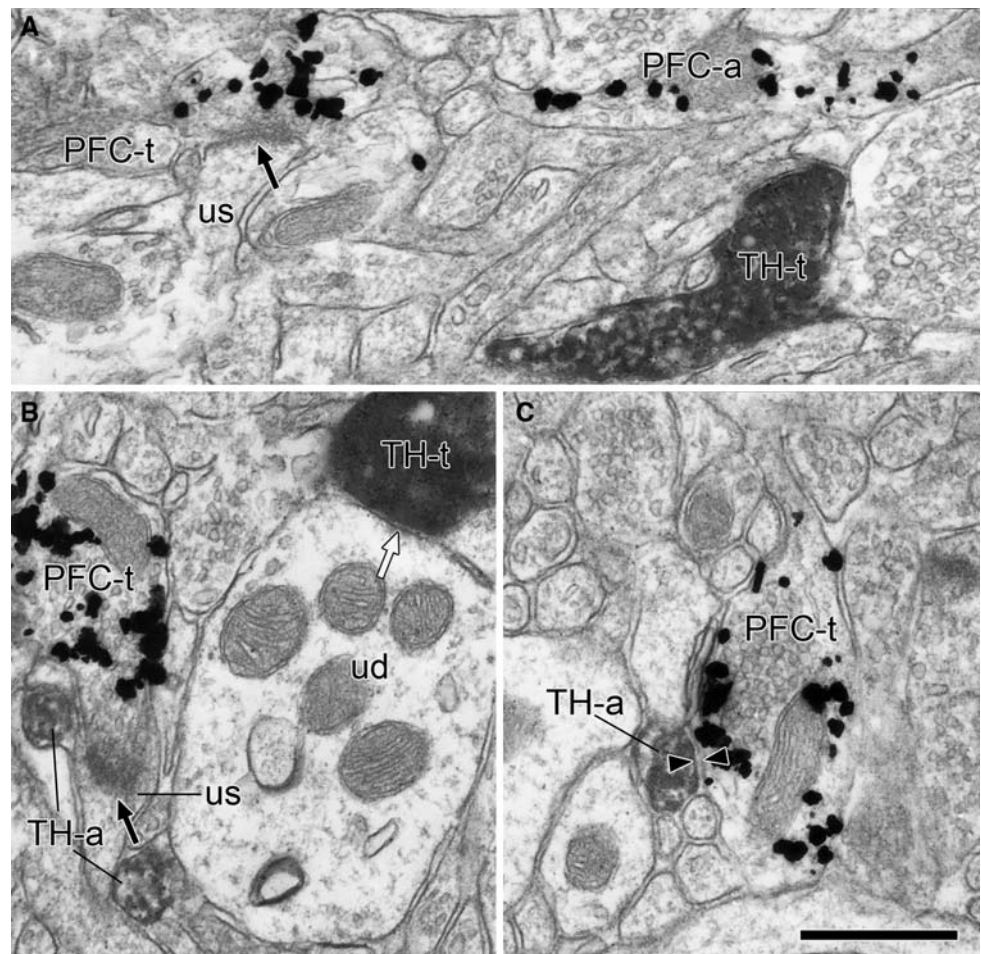
contacted spines that were in apposition to TH-ir profiles (Fig. 3b). As is typical for DA axons in this and other forebrain regions (Asan 1997; Descarries et al. 1996; Sesack 2002; Smiley and Goldman-Rakic 1993), the majority of TH-labeled structures were not observed to form evident synapses in single or a limited series of adjacent sections, although some did form symmetric synapses on spines or dendrites (Fig. 3b). Some PFC terminals were apposed to TH-ir axons (Fig. 3c) without forming synaptic junctions at these points of contact. Finally, examination of single or a short series of sections demonstrated that spines or dendrites receiving PFC synaptic inputs rarely were observed to receive secondary synaptic contacts from other axons, either TH-labeled or unlabeled. However, in one occasion, a PFC terminal synapsed onto a spine, and a TH-ir terminal synapsed onto the dendritic shaft from which the spine emanated (Fig. 4a, b).

Comparisons between the ICMs and BLA

PFC terminals observed within the ICMs or the BLA displayed similar morphology, synaptic incidence (Table 1) and target preference. Within the ICMs, it was more

common to find TH-ir axons in the immediate vicinity of PFC terminals than was observed for the BLA (Table 1). Nevertheless, the frequency with which PFC and TH-ir profiles contacted the same dendritic structures or were apposed to each other was comparable between the two regions (Table 1).

D1R and D2R immunoreactivity within the AMG

At the electron microscopic level, the immunoperoxidase reaction for D1R and D2R was readily recognized as a dark and flocculent precipitate within dendritic and axonal structures (Figs. 5–8) and in rarer instances within glial processes (not shown). D1R immunoreactivity was more readily detectable in the ICMs than the BLA, whereas D2R labeling was equally observed in both structures. The D1R was most commonly found within spines (Fig. 5a, b) that typically received asymmetric synaptic inputs from unlabeled terminals. In some instances, D1R-labeled spines were seen to emerge from parent dendrites that were devoid of D1R labeling (Fig. 5c). The D1R was less commonly present within dendrites (Fig. 5d) or axon terminals (Fig. 5e).
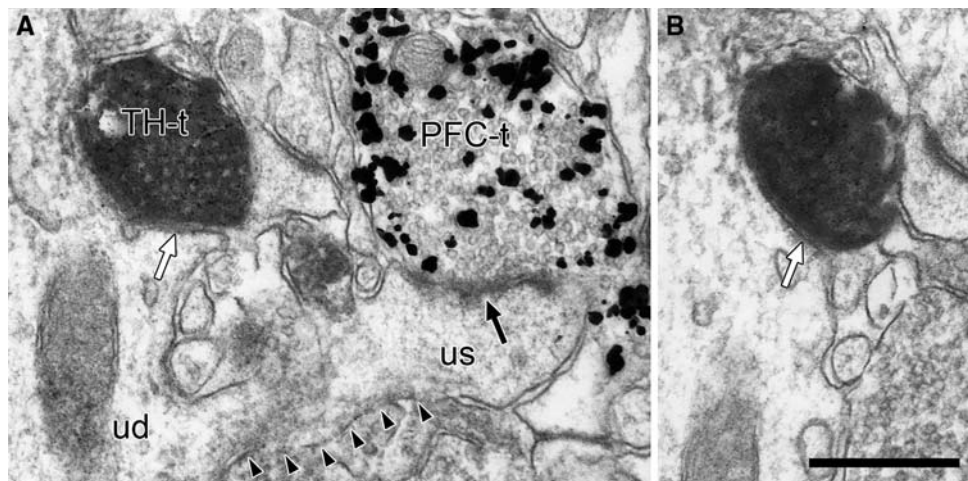
Fig. 4 Serial electron micrographs of a PFC terminal (PFC-t) and a TH-ir terminal (TH-t) synapsing onto the same dendritic structure within the ICMs. In panel **a**, the PFC-t forms an asymmetric synapse (*black arrow*) onto an unlabeled spine (us). The spine emanates from an unlabeled dendrite (ud; the nearly continuous membrane connecting the dendrite and spine can be appreciated along the lower surface as indicated by *arrowheads*), and this dendrite receives a symmetric synapse (*white arrows*) from a TH-t. The serial section in panel **b** better illustrates the synaptic junction formed by the TH-t. *Scale bar* represents 0.5 μm

Fig. 5 Electron micrographs showing immunoperoxidase labeling for the D1 receptor within the ICMs. In panels **a** and **b**, D1-labeled spines (D1-s) receive asymmetric inputs (*black arrows*) from unlabeled terminals (ut). In panel **b**, the *open arrow* indicates D1 labeling within the neck of the spine. In panel **c**, a D1-s appears to emerge from an unlabeled parent dendrite (ud). In panel **d**, a dendrite expresses D1 immunostaining (D1-d), and in panel **e**, a D1-t forms an asymmetric synapse (*black arrow*) onto an unlabeled dendrite. *Scale bar* represents 0.5 μm
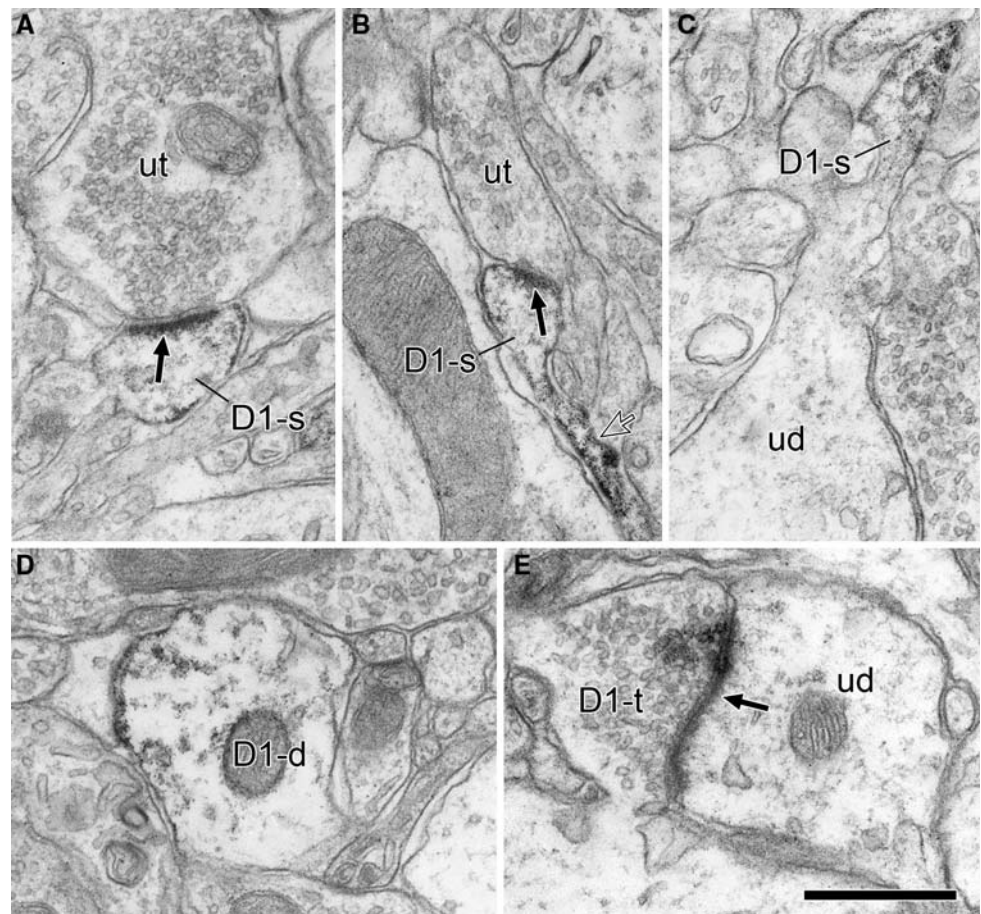
The D2R was frequently observed within dendrites (Fig. 6a, c) and spines (Fig. 6b). In some instances, D2R-labeled spines were seen to emerge from unlabeled dendrites (Fig. 6b). In one case, light immunoperoxidase labeling for the D2R was observed within a dendritic shaft receiving multiple synaptic inputs (Fig. 6c), which is

Fig. 6 Electron micrographs showing immunoperoxidase labeling for the D2 receptor within dendrites (D2-d in panel **a** and **c**), spines (D2-s in panel **b**), and axon terminals (D2-t in panels **d** and **e**) within the ICMs (panels **a** and **d**) and BLA (panels **b**, **c**, and **e**) of the AMG. In panel **b**, the spine exhibits heavy peroxidase labeling for the D2 receptor but emerges from a dendrite that appears to be immunonegative (ud); sa denotes the spine apparatus within the neck. The D2-d in panel **c** contains light peroxidase product (*open arrows*) and has morphological features characteristic of local circuit neurons, specifically the presence of unlabeled terminals (ut) forming multiple symmetric and asymmetric synapses onto the shaft, only some of which are indicated by *white* or *black arrows*, respectively. In panels **d** and **e**, the D2-labeled axonal profiles contain clear vesicles and are either apposed to unlabeled dendrites without synapsing (panel **d**) or form an asymmetric synapse (*black arrow*) onto an unlabeled spine (us in panel **e**). *Scale bar* represents 0.5 μm in panels **a** and **d** and 0.65 μm in panels **b**, **c**, and **e**
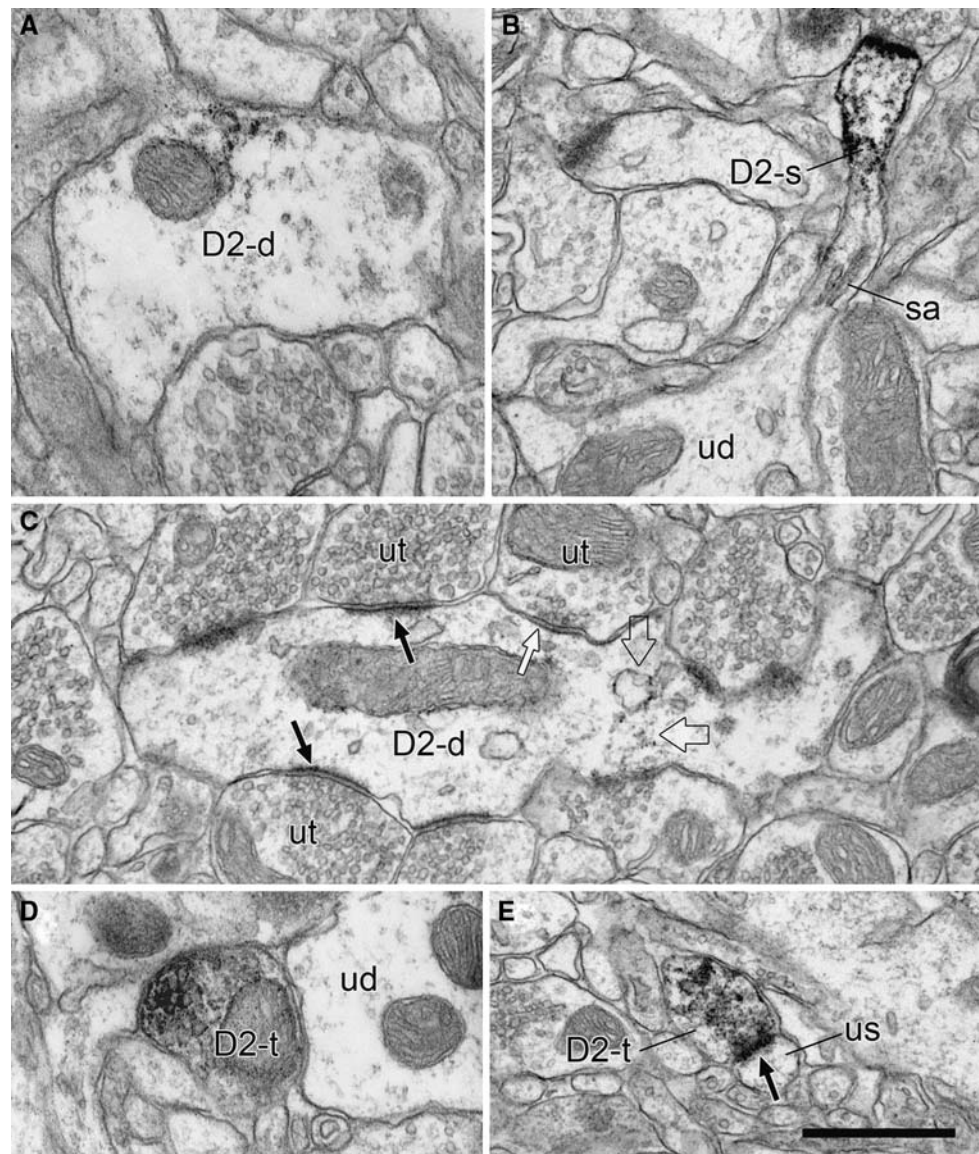
characteristic of local circuit neurons (McDonald et al. 2002). The D2R was frequently found within axonal profiles (Fig. 6d, e). Some of these formed either symmetric or asymmetric synapses (Fig. 6e) onto spines or distal dendrites. Other D2R-labeled axons were not observed to form synapses in single sections (Fig. 6d).

A complete quantitative survey of DA receptor expression in the AMG was beyond the goals of the present study. Moreover, the observations were taken primarily from regions of tissue specifically chosen for their inclusion of axons from the PFC and therefore represent a potentially biased sample. Nevertheless, the limited and semi-quantitative results are provided here in the hope that they might be reflective of the AMG generally. Of 47 structures immunoreactive for the D1R (nearly all of which were from the ICMs), 17 (36%) were dendritic spines, 4 (9%) were

dendritic shafts, 10 (21%) were axons or axon varicosities, and 16 (34%) were unidentified. Of 188 profiles labeled for the D2R (approximately two-thirds of which were from the BLA and one-third from the ICMs), 43 (23%) were spines, 14 (7%) were shafts, 93 (49%) were axons or axon varicosities, and 38 (20%) were unidentified. For either receptor, the unidentified structures were typically small in diameter and therefore most likely intervaricose segments of axons or the necks of dendritic spines.

D1R and D2R spatial relationship to PFC synapses

Within the ICMs, D1R immunolabeled structures were often in the same field as PFC axons (Fig. 7), and PFC terminals occasionally synapsed onto D1R labeled spines (Fig. 7a–c). Out of 168 PFC terminals in this tissue,

Fig. 7 Electron micrographs showing spatial relationships between prefrontal cortical terminals labeled by degeneration (dPFC-t) and D1-labeled structures in the ICMs. In panels **a–c**, dPFC-ts form asymmetric synapses (*black arrows*) onto D1-labeled spines (D1-s). In panel **c**, a dPFC-t synapses simultaneously onto a D1-s and two unlabeled spines (us). In panel **d**, a dPFC-t synapses onto an unlabeled spine, while a nearby D1-s receives synaptic input from an unlabeled terminal (ut) that also synapses onto an unlabeled spine. *Scale bar* represents 0.5 μm
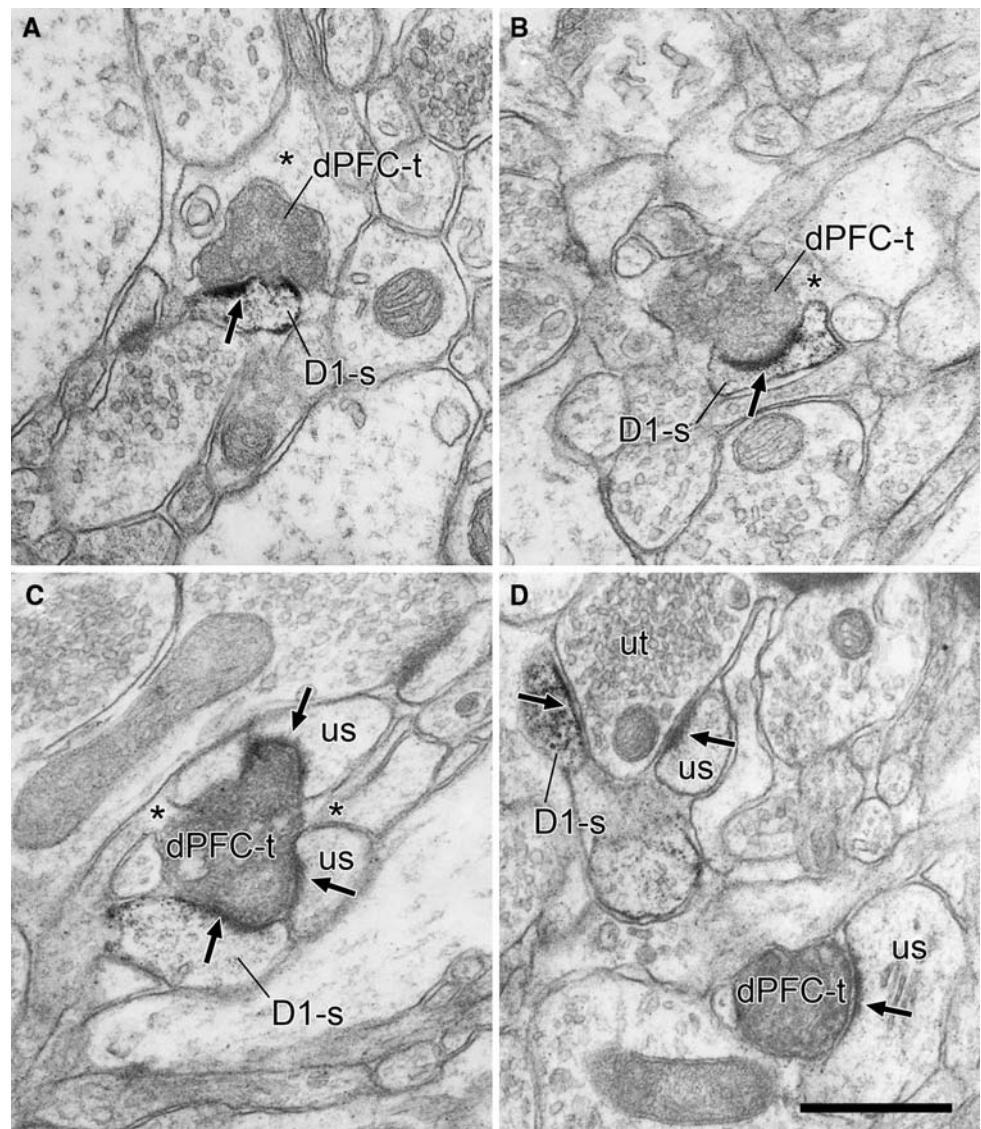
approximately half were observed to form synapses, and of these, roughly 10% synapsed onto D1R labeled spines or dendrites (Table 2). Other PFC terminals synapsed onto spines unlabeled for the D1R (Fig. 7d), and many D1R immunoreactive spines received synaptic input from un-labeled terminals (Fig. 7d). Finally, PFC axons labeled by anterograde tracers were never observed to express immunoreactivity for the D1R.

In tissue labeled for the D2R, PFC and D2R-immuno-labeled structures were also commonly observed in the same field, although they typically were in contact with different structures (Fig. 8a). PFC terminals were never seen to synapse onto D2R-labeled dendrites (Table 2). Nevertheless, approximately 7% of PFC axons and termi-nals expressed immunoreactivity for the D2R (Table 2, Fig. 8). PFC terminals within the BLA and ICMs expressed presynaptic D2R to an equivalent degree.

Discussion

The results of this study provide potential anatomical substrates through which PFC and DA afferents to the AMG might interact. The PFC input targets primarily the ICMs and the BLA and makes predominantly asymmetric synapses onto spines. Dopamine fibers often occupy the neuropil surrounding PFC axons, but in most instances these two afferents have separate synaptic targets. Never-theless, PFC and DA terminals are sometimes apposed to the same dendritic structures, and in rarer instances, these dendrites receive synapses from both sources. Close appositions between PFC and DA axons are also observed. These findings confirm that the PFC provides a direct excitatory influence to neurons within both the ICMs and BLA and suggest that DA modulates PFC drive via pre-dominantly extrasynaptic mechanisms. Consistent with this

Table 2 Spatial relationships between PFC axons and D1/D2 receptor immunoreactivity in the ICMs and BLA

|	D1 ICMs	D2 ICMs	D2 BLA
Total number of PFC axons observed	168	168	88
Number (%) of PFC axons forming synapses	90/168 (54%)	65/168 (39%)	33/88 (38%)
Synapses onto D1/D2+ spines/dendrites	9/90 (10%)	0	0
PFC axons immunoreactive for D1/D2 receptors	0	10/168 (6%)	7/88 (8%)

PFC prefrontal cortex, *ICMs* intercalated cell masses, *BLA* basolateral amygdala

suggestion, D1R staining is present within some of the spines receiving synaptic input from the PFC, and D2R labeling is expressed within a population of PFC axons themselves. Hence, the modulation of PFC transmission in the AMG by D1 receptors is likely to occur primarily via a postsynaptic mechanism, whereas modulation by D2 receptors probably proceeds mainly through a presynaptic influence.

Methodological considerations

In tissue prepared for electron microscopy, immunoreagents do not fully penetrate the tissue, which raises the likelihood of false-negative results. This concern was minimized in the present study by examination of immunolabeled tissue at the superficial region of the sections

Fig. 8 Electron micrographs showing the spatial relationship between prefrontal cortical terminals (PFC-t) and D2-labeled structures in the ICMs. In panel **a**, a PFC-t that contains light immunoreactivity for the D2 receptor (D2 + PFC-t; compare to the two unlabeled terminals in this image) forms an asymmetric synapse (*black arrow*) onto an unlabeled dendrite (ud), while a nearby D2-labeled spine (D2s) is innervated by an unlabeled terminal (ut). In panels **b** and **c**, D2 + PFC-ts synapse onto unlabeled spines (us). *Scale bar* represents 0.5 μm
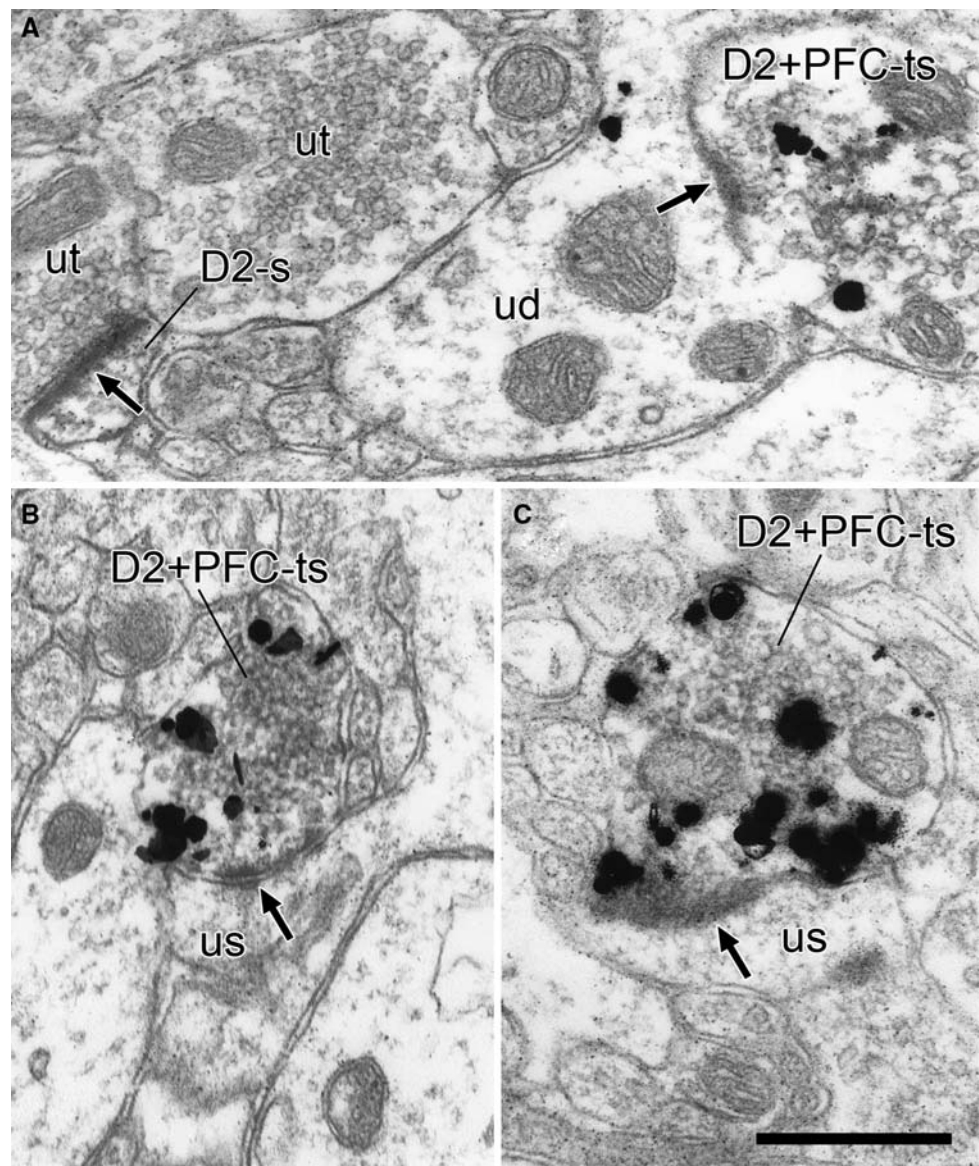
where immunodetection is most probable. Moreover, as discussed earlier, the use of three different tracing methods with distinct advantages and similar outcomes strengthened the veracity of the findings. Hence, although some instances of close convergence of PFC and TH-ir axons onto common targets may have been overlooked, it is likely that such synaptic convergence is infrequent. Moreover, the observation of positive relationships between PFC terminals and D1R and D2R in tissue processed by similar methods substantiates the combined results. Nevertheless, a certain degree of false negative outcomes attends any study of this type, and it is possible that PFC axons have more frequent associations with DA varicosities and/or DA receptors than reported here.

PFC and DA innervation to the AMG

The present light microscopic observations of a dense PFC fiber plexus within the ICMs and dorsomedial BLA agree well with previous descriptions of the PFC projection to the AMG (Berretta et al. 2005; Cassell and Wright 1986; McDonald 1998; McDonald et al. 1996; Sesack et al. 1989; Vertes 2004). Moreover, the ultrastructural findings that PFC terminals target spines (93%) and distal dendritic shafts at asymmetric synapses in both the ICMs and the BLA verifies and extends a prior electron microscopic analysis within the BLA (Brinley-Reed et al. 1995).

PFC afferents to the AMG appear to preferentially target excitatory pyramidal cells within the BLA and inhibitory GABA neurons within the ICMs, although this hypothesis requires direct testing with cell-type specific markers. Pyramidal neurons within the BLA are densely spinous and correspond to 85% of the neuronal population, whereas sparsely-spiny GABA interneurons comprise a smaller group of cells within this complex (McDonald 1992; McDonald et al. 2002; Muller et al. 2006). Hence, the predominance of axo-spinous synapses formed by PFC inputs to the BLA suggests that pyramidal neurons are the principal target (Brinley-Reed et al. 1995). However, electrophysiological data (Rosenkranz and Grace 2002b) indicates that PFC stimulation inhibits pyramidal neuron excitability within the basolateral complex via activation of inhibitory cells. The reason for this discrepancy is not known but may reflect differences in the location of sampling (La in physiology studies versus BLA in the anatomical investigations) as well as differences in the electrotonic strength of PFC synapses onto pyramidal versus local circuit neurons. Within the ICMs, virtually all neurons contain GABA, and most are densely spiny (Millhouse 1986; Nitecka and Ben-Ari 1987) indicating that PFC afferents preferentially innervate spiny projection neurons in the ICMs as they do in the BLA. A recent electrophysiological study indicates that intercalated paracapsular neurons in medial (between the BLA and Ce) and lateral (near the external capsule) sites provide powerful feedforward inhibition to both the BLA and the Ce (Marowsky et al. 2005) [see also commentary by (Pape 2005)]. As the medial paracapsular area is heavily innervated by the PFC, it is possible that the dominant inhibitory action of PFC stimulation on BLA neurons occurs via this mechanism.

The observation that DA processes were most dense within the ICMs, Ce, and basolateral complex agrees with previous descriptions of the DA input to the AMG (Asan 1993; Brinley-Reed and McDonald 1999; Fallon and Ciofi 1992; Marowsky et al. 2005). Moreover, the present ultrastructural findings also match previous reports indicating that DA axons have a relatively low synaptic incidence and target dendrites, spines, and occasionally cell bodies at primarily symmetric synapses (Asan 1997).

Spatial relationships between PFC and DA terminals

No previous studies have described the ultrastructural relationships between PFC and DA afferents to the AMG. Reports that DA receptor activation within the basolateral complex selectively modulates neuronal responses to PFC inputs (Rosenkranz and Grace 1999, 2001) suggest that these afferents operate in close proximity. Moreover, descriptions of DA axons in other brain regions that synapse onto spines receiving convergent inputs from presumed glutamate axons (Freund et al. 1984; Goldman-Rakic et al. 1989; Johnson et al. 1994; Séguéla et al. 1988; Sesack and Pickel 1990, 1992) suggest a potential substrate for DA modulation of PFC transmission in the AMG as well.

The present observation of PFC and DA profiles in close proximity within the AMG suggests that these axons have opportunities to contact common targets or each other. The more frequent detection of such spatial relationships within the ICMs versus the BLA probably reflects a higher PFC and DA innervation density to the former structure. Occasional presynaptic appositions observed between these afferents are consistent with evidence for presynaptic interactions between DA and glutamate in other brain regions (Gracy and Pickel 1996; Morari et al. 1998; Sesack et al. 1994; Sesack and Pickel 1992). Although appositions are not proof of functional interactions, at the least, such close appositions minimize the distance over which transmitters must diffuse in order to exert presynaptic influence. However, the low incidence of synaptic convergence of PFC and DA profiles onto the same small dendrites in the AMG may reflect the fact that DA afferents target mostly dendritic shafts (Asan 1997) and possibly soma (Brinley-Reed and McDonald 1999), whereas PFC terminals synapse mainly onto spines (Brinley-Reed et al. 1995). Hence,

it is important to consider that PFC terminals might innervate spines whose parent dendrites receive synaptic input from DA axons at some distance away. However, this arrangement is more likely to result in DA modulation of general neuronal excitability (Bandyopadhyay et al. 2004; Kröner et al. 2005; Pickel et al. 2006) than specific regulation of PFC synapses (Rosenkranz and Grace 2002b). Moreover, the observation that PFC axons synapse onto spines that rarely receive additional synaptic inputs suggests that DA modulation of PFC inputs to the AMG may involve alternative mechanisms such as 1) indirect actions via either BLA interneurons (Brinley-Reed and McDonald 1999; Rosenkranz and Grace 2001, 2002b) or paracapsular ICM GABA cells (Marowsky et al. 2005), and/or 2) extrasynaptic D1R and D2R localized to PFC profiles or their targets and accessed by DA diffusing from a distant site.

D1R and D2R localization within the AMG

Our light microscopic findings of DA receptor localization within the AMG agree with previous anatomical reports that the D1R is mostly present within the ICMs whereas the D2R is densest within the Ce (Asan 1998; Boyson et al. 1986; Ciliax et al. 1994; Fuxe et al. 2003; Huang et al. 1992; Maltais et al. 2000; Scibilia et al. 1992). Both D1R and D2R are reportedly expressed within the BLA, although in contrast to one prior ultrastructural study (Pickel et al. 2006), examination of the present material revealed that D1R immunoreactivity was notably sparse in the dorsomedial portions of the BLA where PFC afferents are most dense. The reason for this discrepancy with the findings of Pickel and colleagues is not clear, as the same antibody was used in both cases, but it may reflect differences in the immuncytochemical protocol, in particular the higher concentration of antibody used by them.

The presence of mRNA for D1R and D2R within the AMG (Asan 1998; Fremeau et al. 1991; Meador-Woodruff et al. 1991; Weiner et al. 1991) supports our finding that both receptors are present within spines and dendrites of AMG neurons. The observation of immunoreactivity for either receptor within spiny dendrites is consistent with their expression by pyramidal neurons in the BLA and/or spiny cells in the ICMs (McDonald et al. 2002; Millhouse 1986; Nitecka and Ben-Ari 1987). In at least one case, dendritic D2R labeling also appeared in a putative local circuit neuron. These observations agree with physiological reports of postsynaptic DA receptor actions on pyramidal and local circuit neurons in the BLA and GABA cells in the ICMs (Kröner et al. 2005; Lorétan et al. 2004; Marowsky et al. 2005; Pickel et al. 2006; Rosenkranz and Grace 1999, 2001).

Our observation of occasional presynaptic D1R is consistent with a prior electron microscopic study of this receptor in the AMG (Pickel et al. 2006). The localization of D2R on axons and terminals has not been investigated previously in the AMG but is supported by reports of presynaptic D2R in other brain regions (Negyessy and Goldman-Rakic 2005; Sesack et al. 1994; Wang and Pickel 2002) and by possible presynaptic actions of the D2R on GABA neurotransmission in the AMG (Lorétan et al. 2004). For either D1R or D2R, the axons expressing immunoreactivity may be of intrinsic origin or arise from extrinsic sources.

DA receptor relationship to PFC terminals

The finding that D1R labeling was present within spines that received PFC synaptic inputs agrees with electrophysiological data indicating that DA modulates AMG neuronal responses to PFC inputs via postsynaptic activation of D1Rs (Rosenkranz and Grace 2002b) [see also (Pickel et al. 2006)]. However, the latter studies were carried out mainly in the La and BLA, whereas our data regarding D1R localization was collected mainly from the ICMs. Hence, the present findings are most compatible with the proposed model of Marowsky et al., whereby DA acting via D1Rs expressed by paracapsular intercalated neurons facilitates (i.e. disinhibits) neuronal activity in the BLA and Ce evoked by excitatory afferents (Marowsky et al. 2005).

The observation that D2R are localized to PFC axon terminals in the AMG is supported by the presence of D2R mRNA within PFC projection neurons (Gaspar et al. 1995) and is consistent with a similar localization of D2R to PFC axons innervating the striatum (Wang and Pickel 2002). The PFC input to the AMG is topographically organized, with the PL providing a greater input to the BLA than does the IL, whereas both structures project to the ICMs (Cassell and Wright 1986; McDonald 1998; Vertes 2004). The finding of a relatively equivalent proportion of PFC axons dually labeled for the D2R in the BLA and ICMs suggests that the PL and IL innervations to the AMG are under comparable presynaptic D2R modulation.

The spatial relationships between the D2R and PFC terminals in the AMG seem to be exclusively presynaptic, although a possible low level of D2R in the targets of PFC inputs to the AMG cannot be ruled out. Nevertheless, such associations were not observed even in tissue from animals that received the most sensitive tracing method (i.e. anterograde degeneration) combined with the most sensitive immunocytochemical approach for detecting D2R (i.e. ABC immunoperoxidase).

Functional significance

Various studies suggest that an important role of the PFC is the inhibition of maladaptive behaviors (Morgan and

LeDoux 1995; Morgan et al. 1993; Roberts and Wallis 2000). In the AMG, one possible mechanism for this function is the reported influence of the PFC on GABA interneurons within the basolateral complex (Rosenkranz and Grace 2002b), despite the predominant synaptic input of PFC axons to pyramidal cells in this region (Brinley-Reed et al. 1995). Another perhaps more likely mechanism for PFC inhibition of AMG output may be the innervation of the ICMs, which provide a powerful feedforward inhibitory influence (Marowsky et al. 2005) on the two main AMG output stations, the basolateral complex and the Ce (Collins and Pare 1999; Royer et al. 1999). Indeed, the PFC has been reported to mediate a net inhibitory effect on Ce neurons (Quirk et al. 2003), which probably arises via excitation of medial ICM neurons that in turn inhibit Ce cells.

By innervating the structures that receive PFC input, DA has the potential to gate the degree of inhibitory influence mediated from the PFC within the AMG (Marowsky et al. 2005; Rosenkranz and Grace 2002b). Moreover, our demonstration of D1R within PFC synaptic targets and D2R within PFC terminals suggests multiple anatomical substrates for pre- and postsynaptic DA modulation of PFC inputs. Hence, DA receptors appear to be strategically localized to PFC terminals or their targets in a way that facilitates extrasynaptic actions of DA following diffusion from nearby synapses. It is likely that both synaptic and extrasynaptic DA mechanisms are at work within the AMG, such that convergent synaptic inputs, albeit infrequent, provide an immediate, fast and highly localized modulation of PFC responses, and extrasynaptic receptors provide a more tonic influence on overall PFC transmission. In this way, altered DA levels can robustly regulate the excitability of AMG neurons, the degree to which they respond to afferent drive, and the overall strength of synaptic plasticity during emotional learning.

References

Asan E (1997) Ultrastructural features of tyrosine-hydroxylase-immunoreactive afferents and their targets in the rat amygdala. Cell Tissue Res 288:449–469

Asan E (1998) The catecholaminergic innervation of the rat amygdala. Adv Anat Embryol Cell Biol 142:1–119

Asan E (1993) Comparative single and double immunolabelling with antisera against catecholamine biosynthetic enzymes: criteria for the identification of dopaminergic, noradrenergic and adrenergic structures in selected rat brain areas. Histochemistry 99:427–442

Bandyopadhyay S, Gonzalez-Islas C, Hablitz JJ (2004) Dopamine enhances spatiotemporal spread of activity in rat prefrontal cortex. J Neurophysiol 93:864–872

Baxter M, Parker A, Lindner C, Izquierdo A, Murray E (2000) Control of response selection by reinforcer value requires interaction of amygdala and orbital prefrontal cortex. J Neurosci 20:4311–4319

Berretta S, Pantazopoulos H, Caldera M, Pantazopoulos P, Paré D (2005) Infralimbic cortex activation increases c-Fos expression in intercalated neurons of the amygdala. Neuroscience 132:943–953

Boundy VA, Luedtke RR, Artymyshyn RP, Filtz TM, Molinoff PB (1993) Development of polyclonal anti-D2 dopamine receptor antibodies using sequence-specific peptides. Mol Pharmacol 43:666–676

Boyson S, McGonigle P, Molinoff P (1986) Quantitative autoradiographic localization of the D1 and D2 subtypes of dopamine receptors in rat brain. J Neurosci 6:3177–3188

Brinley-Reed M, McDonald AJ (1999) Evidence that dopaminergic axons provide a dense innervation of specific neuronal subpopulations in the rat basolateral amygdala. Brain Res 850:127–135

Brinley-Reed M, Mascagni F, McDonald AJ (1995) Synaptology of prefrontal cortical projections to the basolateral amygdala: an electron microscopic study in the rat. Neurosci Lett 202:45–48

Cassell MD, Wright DJ (1986) Topography of projections from the medial prefrontal cortex to the amygdala in the rat. Brain Res Bull 17:321–333

Ciliax BJ, Hersch SM, Levey AI (1994) Immunocytochemical localization of D1 and D2 receptors in rat brain. In: Niznik HB (ed) Dopamine receptors and transporters: pharmacology, structure and function. Dekker, New York, pp 383–399

Collins DR, Pare D (1999) Reciprocal changes in the firing probability of lateral and central medial amygdala neurons. J Neurosci 19:836–844

Davidson RJ (2002) Anxiety and affective style: role of prefrontal cortex and amygdala. Biol Psychiatry 51:68–80

Davis M (2000) The role of the amygdala in conditioned and unconditioned fear and anxiety. In: Aggleton J (ed) The amygdala—a funtional analysis. Oxford University Press, New York, pp 213–287

Descarries L, Umbriaco D (1995) Ultrastructural basis of monoamine and acetylcholine function in CNS. Semin Neurosci 7:309–318

Descarries L, Watkins KC, Garcia S, Bosler O, Doucet G (1996) Dual character, asynaptic and synaptic, of the dopamine innervation in adult rat neostriatum: a quantitative audoradiographic and immunocytochemical analysis. J Comp Neurol 375:167–186

Drevets WC (2003) Neuroimaging abnormalities in the amygdala in mood disorders. Ann NY Acad Sci 985:420–444

Dumartin B, Caillé I, Gonon F, Bloch B (1998) Internalization of D1 dopamine receptor in striatal neurons in vivo as evidence of activation by dopamine agonists. J Neurosci 18:1650–1661

Fallon J, Ciofi P (1992) Distribution of monoamines within the amygdala. In: Aggleton J (ed) The amygdala: neurobiological aspects of emotion, memory, and mental dysfunction. Wiley-Liss, Inc., New York, pp 97–114

Fremeau R, Duncan G, Fornaretto M-G, Dearry A, Gingrich J, Breese G, Caron M (1991) Localization of D1 dopamine receptor mRNA in brain supports a role in cognitive, affective, and neuroendocrine aspects of dopaminergic transmission. Proc Natl Acad Sci 88:3772–3776

Freund T, Powell J, Smith A (1984) Tyrosine hydroxylase-imunoreactive boutons in synaptic contact with identified striatonigral neurons, with particular reference to denritic spines. Neuroscience 13:1189–1215

Fuxe K, Jacobsen KX, Höistad M, Tinner B, Jansson A, Staines WA, Agnati LF (2003) The dopamine D1 receptor-rich main and

paracapsular intercalated nerve cell groups of the rat amygdala: relationship to the dopamine innervation. Neuroscience 119:733–746

Garcia R, Vouimba RM, Baudry M, Thompson RF (1999) The amygdala modulates prefrontal cortex activity relative to conditioned fear. Nature 402:294–296

Garris P, Wightman R (1994) Different kinetics govern dopaminergic transmission in the amygdala, prefrontal cortex, and striatum: an in vivo voltametric study. J Neurosci 14:442–450

Gaspar P, Bloch B, Le Moine C (1995) D1 and D2 receptor gene expression in the rat frontal cortex: cellular localization in different classes of efferent neurons. Eur J Neurosci 7:1050–1063

Goldman-Rakic PS, Leranth C, Williams SM, Mons N, Geffard M (1989) Dopamine synaptic complex with pyramidal neurons in primate cerebral cortex. Proc Natl Acad Sci 86:9015–9019

Grace AA, Rosenkranz JA (2002) Regulation of conditioned responses of basolateral amygdala neurons. Physiol Behav 77:489–493

Gracy KN, Pickel VM (1996) Ultrastructural immunocytochemical localization of the N-methyl-D-aspartate receptor and tyrosine hydroxylase in the shell of the rat nucleus accumbens. Brain Res 739:169–181

Greba Q, Gifkins A, Kokkinidis L (2001) Inhibition of amygdaloid dopamine D2 receptors impairs emotional learning measured with fear-potentiated startle. Brain Res 899:218–226

Greba Q, Kokkinidis L (2000) Peripheral and intraamygdalar administration of the dopamine D1 receptor antagonist SCH 23390 blocks fear-potentiated startle but not shock reactivity of the shock sensitization of acoustic startle. Behav Neurosci 114:262–272

Guarraci F, Frohardt R, Falls W, Kapp B (2000) The effects of intra-amygdaloid infusions of a D2 dopamine receptor antagonist on Pavlovian fear conditioning. Behav Neurosci 114:647–651

Guarraci FA, Frohardt RJ, Kapp BS (1999) Amygdaloid D1 dopamine receptor involvement in Pavlovian fear conditioning. Brain Res 827:28–40

Hsu SM, Raine L, Fanger H (1981) Use of avidin-biotin-peroxidase complex (ABC) in immunoperoxidase techniques: a comparison between ABC and unlabeled antibody (PAP) procedures. J Histochem Cytochem 29:577–580

Huang Q, Zhou D, Chase K, Gusella J, Aronin N, DiFiglia M (1992) Immunohistochemical localization of the D1 dopamine receptor in rat brain reveals its axonal transport, pre- and postsynaptic localization, and prevalence in the basal ganglia, limbic system, and thalamic reticular nucleus. Proc Natl Acad Sci 89:11988–11992

Inglis FM, Moghaddam B (1999) Dopaminergic innervation of the amygdala is highly responsive to stress. J Neurochem 72:1088–1094

Johnson LR, Aylward RLM, Hussain Z, Totterdell S (1994) Input from the amygdala to the rat nucleus accumbens: its relationship with tyrosine hydroxylase immunoreactivity and identified neurons. Neuroscience 61:851–865

Kröner S, Rosenkranz JA, Grace AA, Barrionuevo G (2005) Dopamine modulates excitability of basolateral amygdala neurons in vitro. J Neurophysiol 93:1598–1610

Lamont EW, Kokkinidis L (1998) Infusion of the dopamine D1 receptor antagonist SCH 23390 into the amygdala blocks fear expression in a potentiated startle paradigm. Brain Res 795:128–136

LeDoux JE (2000) Emotion circuits in the brain. Annu Rev Neurosci 23:155–184

Levey A, Hersch S, Rye D, Sunahara R, Niznik H, Kitt C, Price D, Maggio R, Brann M, Ciliax B (1993) Localization of D1 and D2 dopamine receptors in brain with subtype-specific antibodies. Proc Natl Acad Sci 90:8861–8865

Lewis DA, Sesack SR (1997) Dopamine systems in the primate brain. In: Bloom FE, Björklund A, Hökfelt T (eds) Handbook of chemical neuroanatomy: the primate nervous system, Part 1. Elsevier, Amsterdam, pp 261–373

Lorétan K, Bissière S, Lüthi A (2004) Dopaminergic modulation of spontaneous inhibitory network activity in the lateral amygdala. Neuropharmacology 47:631–639

Maltais S, Coté S, Drolet G, Falardeau P (2000) Cellular colocalization of dopamine D1 mRNA and D2 receptor in rat brain using a D2 dopamine receptor specific polyclonal antibody. Prog Neuropsychopharmacol Biol Psychiatry 24:1127–1149

Marowsky A, Yanagawa Y, Obata K, Vogt KE (2005) A specialized subclass of interneurons mediates dopaminergic facilitation of amygdala function. Neuron 48:1025–1037

McDonald A (1992) Projection neurons of the basolateral amygdala: a correlative golgi and retrograde tract tracing study. Brain Res Bull 28:179–185

McDonald A (1998) Cortical pathways to the mammalian amygdala. Prog Neurobiol 55:257–332

McDonald AJ, Muller JF, Mascagni F (2002) GABAergic innervation of alpha type II calcium/calmodulin-dependent protein kinase immunoreactive pyramidal neurons in the rat basolateral amygdala. J Comp Neurol 446:199–218

McDonald AJ, Mascagni F, Guo L (1996) Projections of the medial and lateral prefrontal cortices to the amygdala: a phaseolus vulgaris leucoagglutinin study in the rat. Neuroscience 71:55–75

Meador-Woodruff JH, Mansour A, Healy DJ, Kuehn R, Zhou Q-Y, Bunzow JR, Akil H, Civelli O, Watson SJ (1991) Comparison of the distributions of D1 and D2 dopamine receptor mRNAs in rat brain. Neuropsychopharmacology 5:231–242

Millhouse OE (1986) The intercalated cells of the amygdala. J Comp Neurol 247:246–271

Miner L, Schroeter S, Blakely R, Sesack S (2003) Ultrastructural localization of the norepinephrine transporter in superficial and deep layers of the rat prelimbic prefrontal cortex and its spatial relationship to probable dopamine terminals. J Comp Neurol 466:478–494

Morari M, Marti M, Sbrenna S, Fuxe K, Bianchi C, Beani L (1998) Reciprocal dopamine-glutamate modulation of release in the basal ganglia. Neurochem Int 33:383–397

Morgan MA, LeDoux JE (1995) Differential contribution of dorsal and ventral medial prefrontal cortex to the acquisition and extinction of conditioned fear in rats. Behav Neurosci 109:681–688

Morgan MA, Romanski LM, LeDoux JE (1993) Extinction of emotional learning: contribution of medial prefrontal cortex. Neurosci Lett 163:109–113

Muller JF, Mascagni F, McDonald AJ (2006) Pyramidal cells of the rat basolateral amygdala: synaptology and innervation by parvalbumin-immunoreactive interneurons. J Comp Neurol 494:635–650

Nader K, LeDoux J (1999) The dopaminergic modulation of fear: quinpirole impairs the recall of emotional memories in rats. Behav Neurosci 113:152–165

Negyessy L, Goldman-Rakic PS (2005) Subcellular localization of the dopamine D2 receptor and coexistence with the calcium-binding protein neuronal calcium sensor-1 in the primate prefrontal cortex. J Comp Neurol 488:464–475

Nitecka L, Ben-Ari Y (1987) Distribution of GABA-like immunoreactivity in the rat amygdaloid complex. J Comp Neurol 266:45–55

Ordronneau P, Lindström P-M, Petrusz P (1981) Four unlabeled antibody bridge techniques: a comparison. J Histochem Cytochem 29:1397–1404

Ottersen OP (1982) Connections of the amygdala of the rat. IV: Corticoamygdaloid and intraamygdaloid connections as studied

with axonal transport of horseradish peroxidase. J Comp Neurol 205:30–48

Pape HC (2005) GABAergic neurons: gate masters of the amygdala, mastered by dopamine. Neuron 48:877–879

Paspalas CD, Goldman-Rakic PS (2004) Microdomains for dopamine volume neurotransmission in primate prefrontal cortex. J Neurosci 24:5292–5300

Paxinos G, Watson C (1986) The rat brain in stereotaxic coordinates. 2nd edn. Academic Press, New York

Peters A, Palay SL, Webster H (1991) The fine structure of the nervous system: neurons and their supporting cells. 3rd edn. Oxford, New York

Phelps EA, Delgado MR, Nearing KI, LeDoux JE (2004) Extinction learning in humans: role of the amygdala and vmPFC. Neuron 43:897–905

Pickel V, Colago E, Mania I, Molosh A, Rainnie D (2006) Dopamine D1 receptors co-distribute with N-methyl-D-aspartic acid type-1 subunits and modulate synaptically-evoked N-methyl-D-aspartic acid currents in rat basolateral amygdala. Neuroscience 142:671–690

Pinto A, Sesack S (2003) Prefrontal cortex projections to the rat amygdala: spatial relationships to dopamine and serotonin afferents. In: Shinnick-Gallagher P, Pitkänen A, Shekhar A, Cahill L (eds) The amygdala in brain function: basic and clinical approaches. New York Academy of Sciences, New York, pp 542–544

Pinto AP, Sesack SR (2000) Limited collateralization of neurons in the rat prefrontal cortex that project to the nucleus accumbens. Neuroscience 97:635–642

Quirk GJ, Likhtik E, Pelletier JG, Paré D (2003) Stimulation of medial prefrontal cortex decreases the responsiveness of central amygdala output neurons. J Neurosci 23:8800–8807

Rauch SL, Shin LM, Wright CI (2003) Neuroimaging studies of amygdala function in anxiety disorders. Ann NY Acad Sci 985:389–410

Roberts AC, Wallis JD (2000) Inhibitory control and affective processing in the prefrontal cortex: neuropsychological studies in the common marmoset. Cereb Cortex 10:252–262

Rosenkranz J, Grace A (2001) Dopamine attenuates prefrontal cortical suppression of sensory inputs to the basolateral amygdala of rats. J Neurosci 21:4090–4103

Rosenkranz J, Grace A (2002a) Dopamine-mediated modulation of odour-evoked amygdala potentials during pavlovian conditioning. Nature 417:282–287

Rosenkranz JA, Grace AA (1999) Modulation of basolateral amygdala neuronal firing and afferent drive by dopamine receptor activation in vivo. J Neurosci 19:11027–11039

Rosenkranz JA, Grace AA (2002b) Cellular mechanisms of infralimbic and prelimbic prefrontal cortical inhibition and dopaminergic modulation of basolateral amygdala neurons in vivo. J Neurosci 22:324–337

Royer S, Martina M, Pare D (1999) An inhibitory interface gates impulse traffic between the input and output stations of the amygdala. J Neurosci 19:10575–10583

Scibilia RJ, Lachowicz JE, Kilts CD (1992) Topographic nonoverlapping distribution of D1 and D2 dopamine receptors in the amygdaloid nuclear complex of the rat brain. Synapse 11:146–154

Séguéla P, Watkins KC, Descarries L (1988) Ultrastructural features of dopamine axon terminals in the anteromedial and suprarhinal cortex of adult rat brain. Brain Res 442:11–22

Sesack S, Aoki C, Pickel V (1994) Ultrastructural localization of D₂ receptor-like immunoreactivity in midbrain dopamine neurons and their striatal targets. J Neurosci 14:88–106

Sesack S (2002) Synaptology of dopamine neurons. In: Chiara GD (ed) Dopamine in the CNS. Springer-Verlag, Berlin, pp 63–119

Sesack SR, Deutch AY, Roth RH, Bunney BS (1989) Topographical organization of the efferent projections of the medial prefrontal cortex in the rat: an anterograde tract-tracing study with Phaseolus vulgaris leucoagglutinin. J Comp Neurol 290:213–242

Sesack SR, Pickel VM (1990) In the rat medial nucleus accumbens, hippocampal and catecholaminergic terminals converge on spiny neurons and are in apposition to each other. Brain Res 527:266–279

Sesack SR, Pickel VM (1992) Prefrontal cortical efferents in the rat synapse on unlabeled neuronal targets of catecholamine terminals in the nucleus accumbens septi and on dopamine neurons in the ventral tegmental area. J Comp Neurol 320:145–160

Sesack SR, Snyder CL, Lewis DA (1995) Axon terminals immunolabeled for dopamine or tyrosine hydroxylase synapse on GABA-immunoreactive dendrites in rat and monkey cortex. J Comp Neurol 363:264–280

Sesack SR, Miner LAH, Omelchenko N (2006) Pre-embedding immunoelectron microscopy: applications for studies of the nervous system. In: Zaborszky L, Wouterlood FG, Lanciego JL (eds) Neuroanatomical tract-tracing 3: molecules, neurons, systems. Springer, New York, pp 6–71

Smiley JF, Goldman-Rakic PS (1993) Heterogeneous targets of dopamine synapses in monkey prefrontal cortex demonstrated by serial section electron microscopy: a laminar analysis using the silver-enhanced diaminobenzidine sulfide (SEDS) immunolabelling technique. Cereb Cortex 3:223–238

Swanson LW (1982) The projections of the ventral tegmental area and adjacent regions: A combined fluorescent retrograde tracer and immunofluorescence study in the rat. Brain Res Bull 9:321–353

Vertes RP (2004) Differential projections of the infralimbic and prelimbic cortex in the rat. Synapse 51:32–58

Veznedaroglu E, Milner TE (1992) Elimination of artifactual labeling of hippocampal mossy fibers seen following pre-embedding immunogold-silver technique by pretreatment with zinc chelator. Microsc Res Tech 23:100–101

Wang H, Pickel VM (2002) Dopamine D2 receptors are present in the prefrontal cortical afferents and their targets in patches of the rat caudate putamen nucleus. J Comp Neurol 442:392–404

Weiner D, Levey A, Sunahara R, Niznik H, O'Dowd B, Seeman P, Brann M (1991) D₁ and D₂ dopamine receptor mRNA in rat brain. Proc Natl Acad Sci 88:1859–1863

Wolf ME, LeWitt PA, Bannon MJ, Dragovic LJ, Kapatos G (1991) Effect of aging on tyrosine hydroxylase protein content and the relative number of dopamine nerve terminals in human caudate. J Neurochem 56:1191–1200

Wouterlood F, Jorritsma-Byham B (1993) The anterograde neuroanatomical tracer biotinylated dextran-amine: comparison with the tracer Phaseolus vulgaris-leucoagglutinin in preparations for electron microscopy. J Neurosci Meth 48:75–87

Yung KK, Bolam JP, Smith AD, Hersch SM, Ciliax BJ, Levey AI (1995) Immunocytochemical localization of D1 and D2 dopamine receptors in the basal ganglia of the rat: light and electron microscopy. Neuroscience 65:709–730